

3-Aryl-1,2,4-oxadiazole Derivatives Active Against Human Rhinovirus

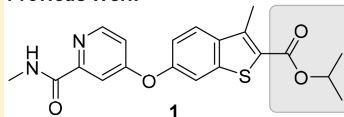
Jinwoo Kim,[†] Jin Soo Shin,[†] Sunjoo Ahn,[†] Soo Bong Han,^{†,‡,Ⓛ} and Young-Sik Jung^{*,†,‡,Ⓛ}[†]Bio & Drug Discovery Division, Korea Research Institute of Chemical Technology, 141 Gajeongro, Yuseong, Daejeon 34114, Republic of Korea[‡]Department of Medicinal Chemistry and Pharmacology, University of Science and Technology, 217 Gajeongro, Yuseong, Daejeon 34113, Republic of Korea

Supporting Information

ABSTRACT: The human rhinovirus (hRV) is the causative agent of the common cold that often aggravates respiratory complications in patients with asthma or chronic obstructive pulmonary disease. The high rate of mutations and variety of serotypes are limiting the development of anti-hRV drugs, which emphasizes the need for the discovery of novel lead compounds. Previously, we identified antiviral compound **1** that we used here as the starting material for developing a novel compound series with high efficacy against hRV-A and -B. Improved metabolic stability was achieved by substituting an ester moiety with a 1,2,4-oxadiazole group. Specifically, compound **3k** exhibited a high efficacy against hRV-B14, hRV-A21, and hRV-A71, with EC₅₀ values of 66.0, 22.0, and 3.7 nM, respectively, and a relevant hepatic stability (59.6 and 40.7% compound remaining after 30 min in rat and human liver microsomes, respectively). An *in vivo* study demonstrated that **3k** possessed a desirable pharmacokinetic profile with low systemic clearance (0.158 L·h⁻¹·kg⁻¹) and modest oral bioavailability (27.8%). Hence, **3k** appears to be an interesting candidate for the development of antiviral lead compounds.

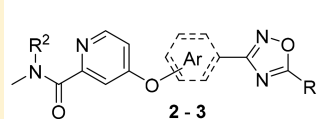
KEYWORDS: Human rhinovirus, capsid-binding, antiviral compound, small molecule inhibitor, oxadiazole

Previous Work



Low metabolic stability
Rat : 0.994
Human : 42.7

Current Work



Ar = benzo[*b*]thiophenyl (**2**),
phenyl (**3**)
R¹ = alkyl
R² = H, methyl

The human rhinovirus (hRV), a member of the *Enterovirus* genus in the *Picornaviridae* family, is a persistent threat to public health. It is known to cause ~60% of upper respiratory tract symptoms such as the common cold. Moreover, recent studies conducted with improved detection methods suggest that hRV infections can aggravate inflammatory illnesses such as asthma, chronic obstructive pulmonary disease, and otitis media.^{1–6} Analyses of viral specimens from pediatric patients with asthma exacerbations identified a high prevalence of hRV.^{7–9} A recent study also revealed that early life hRV wheezing illnesses increase the risk of asthma development at adolescence.¹⁰

More than 160 hRV serotypes have been identified and grouped into three species, hRV-A, -B, and -C, that are each divided into various subspecies.¹¹ Like other picornaviruses, hRV has a positive-sense, single-stranded RNA genome packaged in an icosahedral capsid composed of four viral proteins (VP1 to VP4).¹² The capsid features canyons around its 5-fold symmetry axes that contain binding sites for host receptors such as the intracellular adhesion molecule 1 (ICAM-1), which recognizes most of the hRV subspecies.^{13–15} The neutralizing epitopes, which are hypervariable among the hRV subspecies, are also located along the canyons.^{16–18} In addition, the canyons of several hRV subspecies harbor small molecules, the “pocket factors,” that are probably recovered from the host to facilitate receptor recognition by stabilizing the capsid structure.¹⁹ Receptor binding induces conformational changes

in the capsid to promote its decomposition and enable the injection of the genome into the host cell.²⁰ Viral RNA translation produces a single polyprotein, which is processed into its various parts such as 2A and 3C viral proteases that are crucial for maturation of viral proteins. Subsequent viral replication is accompanied by alterations in the host cell architecture, including rearrangements of the endoplasmic reticulum and Golgi secretory apparatus, although the specific steps vary among subspecies.^{21–23}

Several drug candidates have been developed to combat hRV infections.^{24,25} Capsid-binding inhibitors include pleconaril and vapendavir that associate with the canyon to stabilize the capsid structure, thereby preventing viral genome intrusion.^{26,27} Inhibitors of 3C protease, such as rupintrivir and V-7404, block the maturation of viral proteins,^{28,29} whereas enviroxime, an inhibitor of viral protein 3A, prevents viral replication.³⁰ However, there is a need for the discovery of novel anti-hRV agent candidates because current antiviral drugs are not approved for hRV treatment due to high treatment failure rates and significant side effects.

Recently, we revealed a novel series of small-molecule capsid-binding inhibitors with high effectiveness against replication of

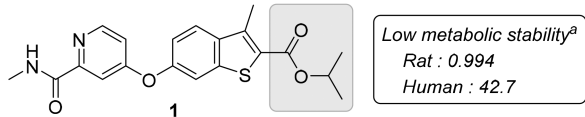
Received: March 21, 2018

Accepted: April 13, 2018

Published: April 13, 2018

hRV-A and -B (Figure 1).³¹ An ester moiety and the high hydrophobicity of the inhibitors represented targets for

Previous Work



Current Work

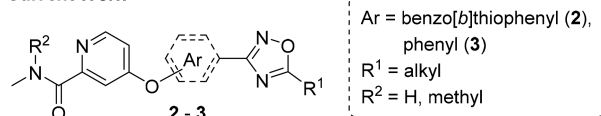
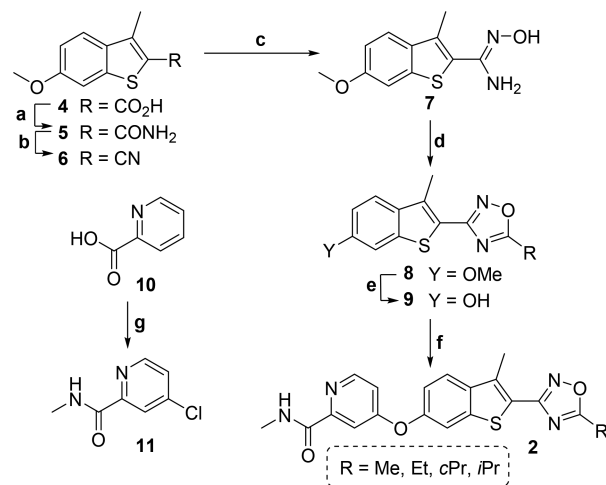


Figure 1. Previously discovered anti-hRV compound (**1**) and new derivatives (**2** and **3**). ^aLiver microsomal stability: amount remaining after 30 min (in percent).

optimization that may lead to improvements in metabolic stability and pharmacokinetics. Here, we hypothesized that these improvements can be achieved by substituting the ester with an oxadiazole moiety. This study describes new 3-aryl-1,2,4-oxadiazole derivatives that exhibit strong activity against hRV-B14, -A21, and -A71, along with significant metabolic stability and hydrophilicity.

The oxadiazole moieties of the new derivatives were prepared from corresponding nitrile groups through cyclization of an *N*-hydroxyimidamide intermediate (Schemes 1 and 2). The

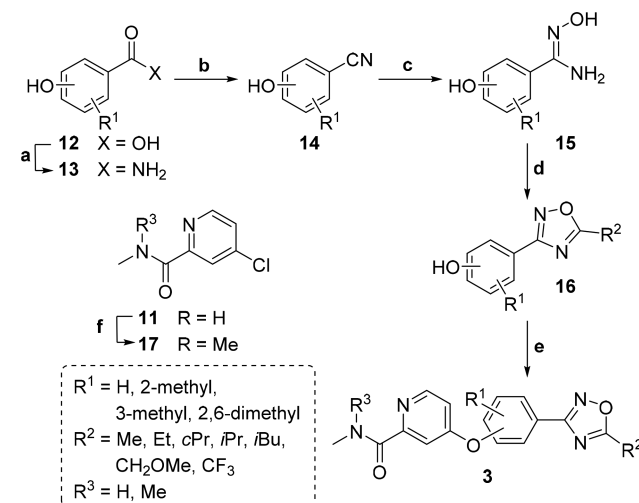
Scheme 1. General Synthetic Route to Benzo[*b*]thiophene Compounds^a



^aReagents and conditions: (a) DMF, SOCl₂, 80 °C, 4 h, then NH₃, H₂O, THF, 0 to 25 °C, 16 h; (b) TFAA, pyridine, ClCH₂CH₂Cl, 25 °C, 1.5 h; (c) NH₂OH, H₂O, EtOH, 90 °C, 48 h; (d) ROCl, pyridine, 0 to 120 °C, 16 h; (e) BBr₃, CH₂Cl₂, -78 to 25 °C, 16 h; (f) **11**, neat, 150 °C, 60 h; (g) DMF, SOCl₂, 45 to 75 °C, 72 h, then CH₃NH₂, H₂O, THF, 0 to 25 °C, 4 h.

benzo[*b*]thiophenyl oxadiazole compounds **2** were synthesized according to the synthetic route outlined in Scheme 1. A reference procedure was employed to synthesize benzo[*b*]thiophene core fragment **4**, which was converted into amide **5** via the acid chloride intermediate using SOCl₂. Amide **5** was further cyanated with trifluoroacetic anhydride (TFAA) and pyridine using chlorinating solvents. Addition of NH₂OH in H₂O–EtOH medium yielded the *N'*-hydroxyimidamide

Scheme 2. General Synthetic Route to Phenyl Compounds^a



^aReagents and conditions: (a) DMF, SOCl₂, 70 °C, 5 h, then NH₃, H₂O, THF, 0 to 25 °C, 16 h; (b) TFAA, pyridine, THF, 0 to 25 °C, 16 h; (c) NH₂OH, H₂O, EtOH, 90 °C, 16 h; (d) RCOCl or TFAA, pyridine, 0 to 120 °C, 16 h; (e) **11** or **17**, neat, 150 °C, 90 h; (f) DMF, SOCl₂, 45 to 75 °C, 72 h, then CH₃NH₂, H₂O, THF, 0 to 25 °C, 4 h; (g) MeI, NaH, DMF, 0 to 25 °C, 3 h.

intermediate **7**. Oxadiazole moieties with diverse alkyl chains were obtained by the cyclization using corresponding acid chlorides. Demethylation of the 6-methoxy mask with BBr₃ exposed the phenolic hydroxyl group for subsequent coupling (**9**). The coupling partner, 4-chloro-*N*-methylpicolinamide (**11**), was generated from picolinic acid **10** by overchlorination in SOCl₂ and DMF followed by amidation. Coupling of **9** and **11** under neat conditions at 150 °C yielded compounds **2** with one exception. The trifluoromethyl compound **2e** was obtained by creating a precoupled amide from **11** and 6-hydroxy-3-methylbenzo[*b*]thiophene-2-carboxamide because of its instability under BBr₃ demethylation condition (see Supporting Information for details).

Although compound **2** derivatives possess a lower hydrophobicity than compound **1** because of the oxadiazole substitution, the new derivatives are extended in length, and additional alkyl length variations of two or more carbon atoms on the oxadiazole ring could significantly interfere in the interaction with one end of the viral capsid canyon. We assumed that changing the benzo[*b*]thiophene core in **2** to phenyl in **3** would not only further increase the hydrophilicity but also provide space for additional variations on the core fragment and the oxadiazole ring. Although the orientation of the oxadiazole ring became distorted, the anti-hRV activities were unlikely to be diminished because, in our previous study, the naphthyl analogs of **1** had also retained activity against hRV-A and -B species.

The synthetic route to phenyl oxadiazole compounds **3** is presented in Scheme 2. *N'*-Hydroxybenzimidamides **15** were obtained from corresponding 4- or 3-hydroxybenzonitriles **14** using NH₂OH. Commercially unavailable benzonitriles were synthesized from hydroxybenzoic acids **12** via the amide intermediates **13**. To obtain **14**, cyanation of **13** was performed using TFAA and pyridine in THF because using the reagents in dichloroethane gave lower yields. Continuing the synthetic route by cyclization of **15** with TFAA or acyl chlorides yielded phenyl oxadiazole cores **16**. 4-Chloro-*N,N*-dimethylpicolinamide

Table 1. Inhibitory Activities of Compounds 2 and 3 against hRVs

Entry	Core structure	Compound	R ¹	R ²	H1HeLa		EC ₅₀ (μM) ^b	
					CC ₅₀ (μM) ^a	hRV14	hRV21	hRV71
1		pleconaril			19.7	0.092	0.073	0.0094
2		2a	Me		>100	0.65	0.059	0.061
3		2b	Et		5.2	0.43	0.077	0.014
4		2c	cPr		6.8	0.47	0.06	0.031
5		2d	iPr		5.5	0.073	0.3	0.013
6		2e	CF ₃		>100	2	0.99	0.3
7			3a	Me	H	>100	33.7	8.7
8	3b		Et	H	43.7	1.1	0.13	0.031
9	3c		cPr	H	32.3	0.52	0.4	0.05
10	3d		iPr	H	16.1	0.073	0.38	0.034
11	3e		iBu	H	23.4	>23.4	2.2	0.34
12	3f		CH ₂ OMe	H	63.4	8.3	2.1	1.7
13	3g		CF ₃	H	35	9.3	>35.0	1.6
14	3h		Et	2-methyl	25.2	0.39	0.23	0.0039
15	3i		cPr	2-methyl	20.0	0.34	0.4	0.012
16	3j		iPr	2-methyl	8.9	0.073	0.029	0.0025
17	3k		iPr	3-methyl	30.5	0.066	0.022	0.0037
18	3l	iPr	2,6-dimethyl	7.4	0.3	0.069	0.011	
19		3m	iPr	H	9	0.28	>9.0	>9.0
20		3n	iPr	2-methyl	1.4	0.49	>1.4	>1.4
21		3o	iPr	2,6-dimethyl	1.8	>1.8	>1.8	>1.8
22		3p	iPr		54.2	12.8	2.1	0.15
23		3q	iBu		19.1	>19.1	2.7	0.37
24		3r	CH ₂ OMe		>100	>100	40.3	2
25		3s	iPr	H	>100	11.5	39.1	6.7
26					6.9	1.7	0.11	0.0084

^aCC₅₀: cytotoxic concentration (μM) that reduced cell viability by 50%; measured in H1HeLa cells using MTT assay. ^bEC₅₀: effective concentration (μM) inhibited hRV replication by 50%; measured in H1HeLa cells using MTT assay.

mid 17 was prepared by methylating 11 using MeI and NaH. The phenolic group of 16 was coupled with 11 or 17 under neat conditions to obtain the desired compounds 3. Because of side reactions during oxadiazole ring formation, the pyridine analog 3s was synthesized using a synthetic route like in Scheme 1. The 6-(oxadiazolyl)naphthalen-2-ol counterpart 3t, however, was synthesized like the phenyl oxadiazole derivatives (see Supporting Information for the details).

The antiviral activities of oxadiazole compounds 2–3 against hRV-B14, -A21, and -A71 were assessed in H1HeLa cells using

the MTT assay with pleconaril as a reference (Table 1). 5-Methyl-1,2,4-oxadiazole derivative 2a, a compound with a molecular volume similar to 1, exhibited activity against the three hRV strains at a nanomolar concentration range (entry 2). Longer and bulkier alkyl substitutions on position 5 of the oxadiazole ring resulted in significantly higher cytotoxicity and slightly improved anti-hRV activity (entries 3–5). Comparing the activities between ethyl-substituted 2b and cyclopropyl-substituted 2c, their activities were similar against hRV-B14, but 2c was much stronger against hRV-A21 than 2b, and

approximately 50% less active against hRV-A71 (entries 3, 4). Assessing the differences between **2b** and isopropyl-substituted **2d**, the activity of **2d** was lower against hRV-B14, higher against hRV-A21, and not different toward hRV-A71 (entry 5). 5-Trifluoromethyl derivative **2e** had low cytotoxicity, but its activity toward the three hRV strains was the lowest among compound **2** variants, implying that electron-richness on the oxadiazole ring is critical for the anti-hRV activities (entry 6).

Anti-hRV activities and cytotoxicity of phenyl oxadiazole derivatives **3a–t** were also assessed. The *para*-substituted phenyl variants **3a–d** and **3g** showed improved cytotoxicity but exhibited mostly lower activities than their respective benzo-*[b]*thiophene counterparts (entries 7–10, 13). Specifically, **3a** had much lower anti-hRV activities than **2a**. Although the tendencies observed for the activities of compounds **3b–d** were similar to their respective counterparts **2b–d**, the activity of **3c** was lower against hRV-21 than against hRV-71, which is the inverse activity pattern observed for **2c**. Furthermore, the extension of the 5-alkyl substitution to isobutyl or methoxymethyl significantly reduced anti-hRV activities, suggesting that derivatives with 5-alkyl substitutions of more than two carbon atoms cannot properly fit into the viral capsid canyon (entries 11, 12). Like **2e**, the CF₃ derivative **3g** exhibited a much lower antiviral activity than **3b–e** (entry 13).

Based on our previous study, we hypothesized that an additional alkyl substitution on the phenyl core of **3** could enhance the interaction between the inhibitor and residue L25 of VP 3, one of the viral capsid constituents.³¹ Addition of a methyl group on the *meta* position toward oxadiazole preserved anti-hRV activities but increased cytotoxicity (entries 14–16). Specifically, an improved anti-hRV21 activity was observed for **3j**, exhibiting EC₅₀ values in the range between 2.5 and 73.0 nM against the three hRV species (entry 16). Further improvement was obtained by adding a methyl group in the *ortho* position toward oxadiazole, which significantly reduced the cytotoxicity (entry 17). Compound **3k** exhibited EC₅₀ values of 66, 22, and 3.7 nM against hRV-B14, -A21, and -A71, respectively. Although the dimethyl derivative **3l** still exhibited high efficacy against hRV-A strains, the activity against hRV-B14 was strongly reduced along with a strong increase in cytotoxicity (entry 18). The *N,N*-dimethylpicolinamide analogs **3m–o** also exhibited high cytotoxicity associated with CC₅₀ values that were no longer above the EC₅₀ values against hRV-A strains (entries 19–21). Variants with *meta*-substituted phenyl core **3p–r** did not exhibit useful antiviral activity profiles, presumably, because these inhibitor molecules are bent, which may prevent the critical hydrophobic interaction between the oxadiazole moiety and the viral pocket (entries 22–24). In addition, the pyridine derivative **3s** with low cytotoxicity showed only moderate antiviral activity (entry 25), whereas the naphthalene derivative **3t** was effective against hRV-A71, but its cytotoxicity was too high for its other modest activities against hRV-B14 and -A21 (entry 26).

The Phase I metabolic stability of selected compounds (**2d**, **3j**, **3k**, and **3l**) was investigated in rat and human liver microsomes (Table 2). The compounds showed higher stability in rat liver microsome than compound **1**. Interestingly, **2d** and **3l** are more stable than **1** in human liver microsome. The most active and least cytotoxic compound **3k** displayed improved Phase I metabolic stability to compound **1**. To elucidate the pharmacokinetics of **3k**, male Sprague–Dawley rats received doses of 5 and 10 mg·kg⁻¹ via the intravenous and oral route, respectively. The **3k** plasma concentration was determined

Table 2. *In Vitro* Liver Microsomal Phase I Stability (% Remaining after 30 min)^a

compound	rat (%)	human (%)
1	1.0 ± 0.1	42.7 ± 0.6
2d	99.2 ± 0.3	69.8 ± 8.9
3j	35.1 ± 6.3	9.9 ± 3.1
3k	59.6 ± 5.7	40.7 ± 1.0
3l	37.1 ± 2.6	61.1 ± 3.7
bupirone	0.1 ± 0.01	3.5 ± 0.5

^aEach value is presented as mean ± standard deviation of at least three independent experiments.

using LC–MS/MS after sample deproteinization in acetonitrile (Figure 2). The plasma concentration–time data were analyzed

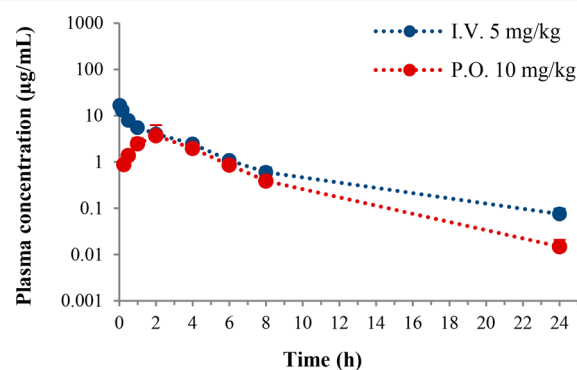


Figure 2. Plasma concentration–time profiles of **3k** in male rats ($n = 3$).

by applying the noncompartmental method using Phoenix WinNonlin (v6.4; Pharsight Corp., Mountain View, CA, USA). After intravenous dosing, the AUC_t value at 5 mg·kg⁻¹ was 31.3 µg·h·mL⁻¹ along with a low systemic clearance rate of 0.158 L·h⁻¹·kg⁻¹. After the oral administration, **3k** was slowly absorbed and reached a C_{max} of 3.9 µg·mL⁻¹. Then, the **3k** plasma concentrations declined with a terminal T_{1/2} of 3.2 h. The systemic exposure (AUC_t) following an oral dose was 17.4 µg·h·mL⁻¹ and the oral bioavailability was 27.8% (Table 3).

Table 3. Pharmacokinetics of **3k** in Male Rats^a

parameter	I.V., 5 mg·kg ^{-1b}	P.O., 10 mg·kg ^{-1c}
T _{max} (h)	NA	2.7 ± 1.2
C _{max} (µg·mL ⁻¹)	NA	3.9 ± 2.4
T _{1/2} (h)	4.6 ± 1.1	3.2 ± 0.4
AUC _t (µg·h·mL ⁻¹)	31.3 ± 2.5	17.4 ± 5.4
AUC _∞ (µg·h·mL ⁻¹)	31.8 ± 2.8	17.4 ± 5.4
CL (L·h ⁻¹ ·kg ⁻¹)	0.158 ± 0.014	NA
V _{SS} (L·kg ⁻¹)	0.611 ± 0.029	NA
F _t (%)	NA	27.8

^aEach value is presented as mean ± standard deviation of at least three independent experiments. ^bParameters from intravenous administration. ^cParameters from oral administration.

In this study, we used antiviral compound **1** as starting material for developing two novel compound series, derivatives **2** and **3**, that we examined for their inhibitory activity against hRV-B14, -A21, and -A71. We showed that substituting the ester moiety of compound **1** by a 1,2,4-oxadiazole group in **2** and **3** created molecules with antiviral activity and significant

metabolic stability. Several compounds were highly active with EC_{50} values in the nanomolar range against the three hRV species. Specifically, compound **3k** displayed a high efficacy against hRV-B14, hRV-A21, and hRV-A71, with EC_{50} values of 66.0, 22.0, and 3.7 nM, respectively. In addition, the hepatic stability of **3k** was better than compound **1** in rat microsomes and similar for both compounds in human microsomes. A pharmacokinetics analysis of **3k** in rats demonstrated that the inhibitor had a low systemic clearance and a moderate oral bioavailability. Hence, **3k** represents an interesting candidate for the development of novel antiviral lead compounds.

■ ASSOCIATED CONTENT

Supporting Information

The Supporting Information is available free of charge on the ACS Publications website at DOI: [10.1021/acsmchemlett.8b00134](https://doi.org/10.1021/acsmchemlett.8b00134).

Detailed synthetic procedures and UPLC purity and characterization data for compounds **2–3**, including the spectral copies of ^1H and ^{13}C NMR spectra (PDF)

■ AUTHOR INFORMATION

Corresponding Author

*E-mail: ysjung@kriect.re.kr.

ORCID

Soo Bong Han: 0000-0002-7831-1832

Young-Sik Jung: 0000-0001-9492-6848

Notes

The authors declare no competing financial interest.

■ ACKNOWLEDGMENTS

This study was supported by Korea Research Institute of Chemical Technology (Grant No. KK1703-C00, KK1703-E00, and KK1803-D00).

■ ABBREVIATIONS

AUC_t , areas under the plasma concentration–time curve; AUC_{∞} , areas under the plasma concentration–time curve from time zero; CL, total clearance from plasma; C_{max} , maximum plasma concentration; DMF, dimethylformamide; F_t , bioavailability; hRV, human rhinovirus; ICAM-1, intracellular adhesion molecule 1; MTT, 3-(4,5-dimethylthiazol-2-yl)-2,5-diphenyltetrazolium bromide; TFAA, trifluoroacetic anhydride; THF, tetrahydrofuran; T_{max} , time of maximum drug concentration; $T_{1/2}$, terminal half-life; VP, viral capsid protein; V_{ss} , steady-state volume of distribution

■ REFERENCES

- (1) George, S. N.; Garcha, D. S.; Mackay, A. J.; Patel, A. R.; Singh, R.; Sapsford, R. J.; Donaldson, G. C.; Wedzicha, J. A. Human rhinovirus infection during naturally occurring COPD exacerbations. *Eur. Respir. J.* **2014**, *44*, 87–96.
- (2) Gern, J. E. How rhinovirus infections cause exacerbations of asthma. *Clin. Exp. Allergy* **2015**, *45*, 32–42.
- (3) Johnston, S. L.; Sanderson, G.; Pattermore, P. K.; Smith, S.; Bardin, P. G.; Bruce, C. B.; Lambden, P. R.; Tyrrell, D. A.; Holgate, S. T. Use of polymerase chain reaction for diagnosis of picornavirus infection in subjects with and without respiratory symptoms. *J. Clin. Microbiol.* **1993**, *31*, 111–117.
- (4) Mallia, P.; Message, S. D.; Gielen, V.; Contoli, M.; Gray, K.; Kebadze, T.; Aniscenko, J.; Laza-Stanca, V.; Edwards, M. R.; Slater, L.; Papi, A.; Stanciu, L. A.; Kon, O. M.; Johnson, M.; Johnston, S. L.

Experimental rhinovirus infection as a human model of chronic obstructive pulmonary disease exacerbation. *Am. J. Respir. Crit. Care Med.* **2011**, *183*, 734–742.

- (5) Message, S. D.; Laza-Stanca, V.; Mallia, P.; Parker, H. L.; Zhu, J.; Kebadze, T.; Contoli, M.; Sanderson, G.; Kon, O. M.; Papi, A.; Jeffery, P. K.; Stanciu, L. A.; Johnston, S. L. Rhinovirus-induced lower respiratory illness is increased in asthma and related to virus load and Th1/2 cytokine and IL-10 production. *Proc. Natl. Acad. Sci. U. S. A.* **2008**, *105*, 13562.

- (6) Seppala, E.; Sillanpaa, S.; Nurminen, N.; Huhtala, H.; Toppari, J.; Ilonen, J.; Veijola, R.; Knip, M.; Sipila, M.; Laranne, J.; Oikarinen, S.; Hyoty, H. Human enterovirus and rhinovirus infections are associated with otitis media in a prospective birth cohort study. *J. Clin. Virol.* **2016**, *85*, 1–6.

- (7) Heymann, P. W.; Carper, H. T.; Murphy, D. D.; Platts-Mills, T. A.; Patrie, J.; McLaughlin, A. P.; Erwin, E. A.; Shaker, M. S.; Hellem, M.; Peerzada, J.; Hayden, F. G.; Hatley, T. K.; Chamberlain, R. Viral infections in relation to age, atopy, and season of admission among children hospitalized for wheezing. *J. Allergy Clin. Immunol.* **2004**, *114*, 239–247.

- (8) Khetsuriani, N.; Kazerouni, N. N.; Erdman, D. D.; Lu, X.; Redd, S. C.; Anderson, L. J.; Teague, W. G. Prevalence of viral respiratory tract infections in children with asthma. *J. Allergy Clin. Immunol.* **2007**, *119*, 314–321.

- (9) Rawlinson, W. D.; Waliuzzaman, Z.; Carter, I. W.; Belessis, Y. C.; Gilbert, K. M.; Morton, J. R. Asthma exacerbations in children associated with rhinovirus but not human metapneumovirus infection. *J. Infect. Dis.* **2003**, *187*, 1314–1318.

- (10) Rubner, F. J.; Jackson, D. J.; Evans, M. D.; Gangnon, R. E.; Tisler, C. J.; Pappas, T. E.; Gern, J. E.; Lemanske, R. F., Jr Early life rhinovirus wheezing, allergic sensitization, and asthma risk at adolescence. *J. Allergy Clin. Immunol.* **2017**, *139*, 501–507.

- (11) Palmberg, A. C.; Spiro, D.; Kuzmickas, R.; Wang, S.; Djikeng, A.; Rathe, J. A.; Fraser-Liggett, C. M.; Liggett, S. B. Sequencing and Analyses of All Known Human Rhinovirus Genomes Reveal Structure and Evolution. *Science* **2009**, *324*, 55.

- (12) Rossmann, M. G.; Arnold, E.; Erickson, J. W.; Frankengerger, E. A.; Griffith, J. P.; Hecht, H. J.; Johnson, J. E.; Kamer, G.; Luo, M.; Mosser, A. G.; et al. Structure of a human common cold virus and functional relationship to other picornaviruses. *Nature* **1985**, *317*, 145–153.

- (13) Colonna, R. J.; Condra, J. H.; Mizutani, S.; Callahan, P. L.; Davies, M. E.; Murcko, M. A. Evidence for the direct involvement of the rhinovirus canyon in receptor binding. *Proc. Natl. Acad. Sci. U. S. A.* **1988**, *85*, 5449–5453.

- (14) Hofer, F.; Gruenberger, M.; Kowalski, H.; Machat, H.; Huettinger, M.; Kuechler, E.; Blass, D. Members of the low density lipoprotein receptor family mediate cell entry of a minor-group common cold virus. *Proc. Natl. Acad. Sci. U. S. A.* **1994**, *91*, 1839–1842.

- (15) Staunton, D. E.; Merluzzi, V. J.; Rothlein, R.; Barton, R.; Marlin, S. D.; Springer, T. A. A cell adhesion molecule, ICAM-1, is the major surface receptor for rhinoviruses. *Cell* **1989**, *56*, 849–853.

- (16) Glanville, N.; Johnston, S. L. Challenges in developing a cross-serotype rhinovirus vaccine. *Curr. Opin. Virol.* **2015**, *11*, 83–88.

- (17) Skern, T.; Neubauer, C.; Frasel, L.; Grundler, P.; Sommergruber, W.; Zorn, M.; Kuechler, E.; Blass, D. A neutralizing epitope on human rhinovirus type 2 includes amino acid residues between 153 and 164 of virus capsid protein VP2. *J. Gen. Virol.* **1987**, *68*, 315–323.

- (18) Smith, T. J.; Chase, E. S.; Schmidt, T. J.; Olson, N. H.; Baker, T. S. Neutralizing antibody to human rhinovirus 14 penetrates the receptor-binding canyon. *Nature* **1996**, *383*, 350–354.

- (19) Lewis, J. K.; Bothner, B.; Smith, T. J.; Siuzdak, G. Antiviral agent blocks breathing of the common cold virus. *Proc. Natl. Acad. Sci. U. S. A.* **1998**, *95*, 6774–6778.

- (20) Reisdorph, N.; Thomas, J. J.; Katpally, U.; Chase, E.; Harris, K.; Siuzdak, G.; Smith, T. J. Human rhinovirus capsid dynamics is controlled by canyon flexibility. *Virology* **2003**, *314*, 34–44.

(21) Belov, G. A.; Ehrenfeld, E. Involvement of cellular membrane traffic proteins in poliovirus replication. *Cell Cycle* **2007**, *6*, 36–38.

(22) Mousnier, A.; Swieboda, D.; Pinto, A.; Guedán, A.; Rogers, A. V.; Walton, R.; Johnston, S. L.; Solari, R. Human Rhinovirus 16 Causes Golgi Apparatus Fragmentation without Blocking Protein Secretion. *J. Virol.* **2014**, *88*, 11671–11685.

(23) Quiner, C. A.; Jackson, W. T. Fragmentation of the Golgi apparatus provides replication membranes for human rhinovirus 1A. *Virology* **2010**, *407*, 185–195.

(24) De Palma, A. M.; Vliegen, I.; De Clercq, E.; Neyts, J. Selective inhibitors of picornavirus replication. *Med. Res. Rev.* **2008**, *28*, 823–884.

(25) Patick, A. K. Rhinovirus chemotherapy. *Antiviral Res.* **2006**, *71*, 391–396.

(26) Diana, G. D.; Rudewicz, P.; Pevear, D. C.; Nitz, T. J.; Aldous, S. C.; Aldous, D. J.; Robinson, D. T.; Draper, T.; Dutko, F. J.; Aldi, C.; et al. Picornavirus inhibitors: trifluoromethyl substitution provides a global protective effect against hepatic metabolism. *J. Med. Chem.* **1995**, *38*, 1355–1371.

(27) Feil, S. C.; Hamilton, S.; Krippner, G. Y.; Lin, B.; Luttick, A.; McConnell, D. B.; Nearn, R.; Parker, M. W.; Ryan, J.; Stanislawski, P. C.; Tucker, S. P.; Watson, K. G.; Morton, C. J. An Orally Available 3-Ethoxybenzoxazole Capsid Binder with Clinical Activity against Human Rhinovirus. *ACS Med. Chem. Lett.* **2012**, *3*, 303–307.

(28) Dragovich, P. S.; Prins, T. J.; Zhou, R.; Webber, S. E.; Marakovits, J. T.; Fuhrman, S. A.; Patick, A. K.; Matthews, D. A.; Lee, C. A.; Ford, C. E.; Burke, B. J.; Rejto, P. A.; Hendrickson, T. F.; Tuntland, T.; Brown, E. L.; Meador, J. W., 3rd; Ferre, R. A.; Harr, J. E.; Kosa, M. B.; Worland, S. T. Structure-based design, synthesis, and biological evaluation of irreversible human rhinovirus 3C protease inhibitors. 4. Incorporation of P1 lactam moieties as L-glutamine replacements. *J. Med. Chem.* **1999**, *42*, 1213–1224.

(29) Patick, A. K.; Brothers, M. A.; Maldonado, F.; Binford, S.; Maldonado, O.; Fuhrman, S.; Petersen, A.; Smith, G. J., 3rd; Zalman, L. S.; Burns-Naas, L. A.; Tran, J. Q. In vitro antiviral activity and single-dose pharmacokinetics in humans of a novel, orally bioavailable inhibitor of human rhinovirus 3C protease. *Antimicrob. Agents Chemother.* **2005**, *49*, 2267–2275.

(30) Wikel, J. H.; Paget, C. J.; DeLong, D. C.; Nelson, J. D.; Wu, C. Y.; Paschal, J. W.; Dinner, A.; Templeton, R. J.; Chaney, M. O.; Jones, N. D.; Chamberlin, J. W. Synthesis of syn and anti isomers of 6-[[[(hydroxyimino)phenyl]methyl]-1-[(1-methylethyl)sulfonyl]-1H-benzimidazol-2-amine. Inhibitors of rhinovirus multiplication. *J. Med. Chem.* **1980**, *23*, 368–372.

(31) Kim, J.; Jung, Y. K.; Kim, C.; Shin, J. S.; Scheers, E.; Lee, J. Y.; Han, S. B.; Lee, C. K.; Neyts, J.; Ha, J. D.; Jung, Y. S. A Novel Series of Highly Potent Small Molecule Inhibitors of Rhinovirus Replication. *J. Med. Chem.* **2017**, *60*, 5472–5492.